Vibrational Optical Activity Study of *trans*-Succinic-d_2 Anhydride

Petr Bouř,[†,‡] Cheok N. Tam,[†,§] Mohammad Shaharuzzaman,[||] James. S. Chickos,[||] and Timothy A. Keiderling*[,†]

Department of Chemistry (M/C 111), University of Illinois at Chicago, 845 W. Taylor Street, Chicago, Illinois 60607-7061, Institute of Organic Chemistry and Biochemistry, Academy of Sciences of the Czech Republic, 16610 Prague 6, Czech Republic, and Department of Chemistry, University of Missouri St. Louis, 8001 Natural Bridge Road, St. Louis, Missouri 63121

Received: April 30, 1996; In Final Form: June 20, 1996[⊗]

The (*R*-,*R*-) and (*S*-,*S*-) enantiomers of the *trans*-dideuteriosuccinic anhydride were synthesized, and their infrared absorption, vibrational circular dichroism (VCD), and Raman spectra were measured. *Ab initio* quantum mechanical harmonic force fields (FFs) were calculated at the SCF (6-31G**), MP2, and density functional (DFT) levels, transition frequencies were generated, and the fundamental vibrational transitions were assigned. Anharmonic corrections to the SCF and DFT FFs were generated using numerical differentiation to obtain cubic and selected quartic terms. Good overall agreement was observed for the vibrational frequencies and the IR absorption intensities between experimental and calculated results. Computations of the Raman and VCD intensities were carried out at the SCF level, the latter using the magnetic field perturbation method of Stephens and co-workers. The computed Raman intensities are in qualitative agreement with the main experimental features. For the mid-IR VCD transitions, full sign agreement was obtained between the experiment and computations for the (*S*,*S*) isomer, enabling the absolute configuration of the title compound to be determined unambiguously.

Introduction

Vibrational circular dichroism (VCD) can be calculated for a number of small molecules using the magnetic field perturbation (MFP) model as formulated by Stephens.[1] We have applied it on the *ab initio* quantum mechanical self-consistent field (SCF) level to several model systems made chiral by deuteration, such as (3*R*,4*R*)-3,4-dideuteriocyclobutane-1,2-dione[2] and (2*S*,3*S*)-2,3-dideuteriobutyrolactone.[3] For those cases, however, scaling of the harmonic force field was necessary to achieve a reasonable agreement between simulated and experimental VCD spectra. Such a scaling is possibly problematic for molecules with a more complex electronic structure and for vibrational modes affected by Fermi resonances. In this paper, we focus on succinic anhydride, a relatively small molecule which has two coupled localized π-systems (the C═O groups bridged by an O). To improve the accuracy of the *ab initio* calculations, we used the MP2 level of CI correction and density functional theory (DFT) to obtain more accurate molecular force fields and atomic polar tensors and then calculated the atomic axial tensors separately on the SCF level, following methods proposed by Stephens and co-workers.[4] In addition, using our recently developed theoretical methods,[5,6] we calculated anharmonic corrections to the molecular force field as well as to the dipolar electric and magnetic derivatives.

trans-Dideuteriosuccinic anhydride is a rigid molecule, and, because of its symmetry (C_2; C_{2V} for the electronic energy and force field calculations, which are done on the d_0 species), it is possible to carry out high-precision *ab initio* calculations for this anhydride. There is a strong coupling between the carbonyl vibrations, caused by the electronic resonance, as was first observed for maleic anhydride.[7] Vibrational modes of the nondeuterated isomer have been previously assigned on the basis of vapor phase spectra and an empirical force field.[8]

Part of our goal in continuing to study theoretical simulation of the IR absorption and VCD spectra of model compounds is the hope that efforts spent on thorough studies of smaller systems should pay off in future spectral/structural studies of (generally larger) biologically important molecules. Our previous results from computation of the VCD spectra for model peptides[9] encourage our effort to extend *ab initio* calculations toward larger systems. With the latest computational approaches, particularly with the implementations of the density functional theory, good molecular force fields can be obtained for such systems at an approachable computer cost.[4,10]

Experimental Section

Synthesis. Both (2*R*,3*R*)- and (2*S*,3*S*)-succinic-2,3-d_2 anhydrides were synthesized from the corresponding succinic acids by treatment with acetyl chloride.[11] As starting reagents, (2*R*,3*R*)- and (2*S*,3*S*)-2,3-dideuteriosuccinic acid were prepared in a 63% ± 10% enantiomeric excess as has been reported separately.[12] In brief, the chiral acids were obtained by a reduction of the half-acid ester of ethyl fumarate with D_2 in the presence of catalytic amounts of (*R*)- or (*S*)-BINAP Ru(II) diacetate complex to yield the half-ester of (2*R*,3*R*)- or (2*S*,3*S*)-succinic-2,3-d_2 acid, respectively. Conversion to the respective succinic acids gave the starting materials whose optical purity was determined by measurement of their electronic CD spectra in the far-UV of the acid and comparison to previous preparations of known optical purity.[12] After dehydration, the two enantiomers of the anhydride were purified by sublimation. Back hydrolysis to the acid was used to show that the anhydride suffered no loss of enantiomeric excess.

Spectroscopy. The VCD instruments used here have been discussed in detail in the literature.[14] VCD and IR absorption spectra were measured on an FTIR (BioRad Digilab FTS-60A)

* To whom inquiries should be addressed at UIC.
† University of Illinois at Chicago.
‡ Academy of Sciences of theCzech Republic, permanent address.
§ Present address: IPNS Division, Argonne National Laboratory, B-360, 9700 S. Cass Ave., Argonne, IL 60439.
|| University of Missouri.
⊗ Abstract published in *Advance ACS Abstracts,* August 15, 1996.

S0022-3654(96)01217-8 CCC: $12.00

based spectrometer in the mid-IR region (1600−800 cm^{-1}) at a resolution of 4 cm^{-1}, using a BaF_2 substrate grid polarizer, a ZnSe modulator (Hinds), and ZnSe focusing lens. The absorbances of the C−H and C−D stretch regions were also obtained with the same FTIR, but attempts to measure the VCD in this region with this spectrometer were unsuccessful due to the very low extinction coefficients for these bands. The VCD spectrum of the C═O stretch was remeasured using a dispersive instrument at 10 cm^{-1} resolution, with a BaF_2 substrate grid polarizer (Cambridge Physical Sciences), CaF_2 modulator (Hinds), and CaF_2 focusing lens. In all cases, VCD spectra of the other enantiomer were obtained and subtracted from the sample spectrum to correct the base line and improve the signal-to-noise (S/N) ratio. Calibration of the VCD was done with our usual techniques.[14] Absorption base lines were obtained with the same sample cell containing just solvent.

Raman spectra of the title compound have been measured using a Raman spectrometer assembled in house,[15] in both 180° and 90° scattering geometries for unpolarized, polarized, and depolarized Raman spectra. The primary elements of the spectrometer consist of an Ar-ion laser (Coherent, Innova 300), a 0.64 m single spectrograph (ISA J-Y 640), and an intensified diode array detector (PAR 1420 with an OMA III controller). A slit width of 100 μm and a 600 groove/mm grating were used to yield a resolution of 8−10 cm^{-1} in the 180° backscattering experiments, while a 250 μm slit width and a 1800 groove/mm grating were used to give a resolution of 6−8 cm^{-1} in the 90° scattering experiments. A holographic notch filter (Kaiser) enabled detection of reasonable Raman spectra down to 150 cm^{-1}. Attempts to collect ROA (Raman optical activity) spectra on these samples were unsuccessful because the Raman-scattering intensities due to the sample were much weaker than those from the solvent even when a saturated solution of the sample was used. Thus, any true ROA signals that might have been observed had very low S/N and were subject to severe interference by the residual ROA artifacts from the strongly polarized Raman bands of the solvent.

For the mid-IR region VCD and IR spectra, solution samples were prepared by dissolving the succinic anhydride in $CDCl_3$ and in $CHCl_3$ at 5 mg/mL (∼0.05 M) and for the C═O stretch in $CDCl_3$ at 2 mg/mL (∼0.02 M). In both cases the sample was placed in a variable path length cell with KBr windows (Wilks), and spectra were obtained using a 0.5 mm path length. Due to the weak IR intensities of those stretching bands, near saturated solutions in acetone and acetone-d_6 were made up for study of the C−D and C−H stretching region spectra, respectively, using a 1.0 mm path length. Since the amount of the optically active samples was limited, samples used in later experiments were recovered from those prepared for the earliest experiments.

For sake of comparison to previous literature studies,[8] the absorption spectrum of the anhydride vapor was measured in a brass cell with KBr windows, having a 100 mm path length, at a resolution of 0.1 cm^{-1}. Solid succinic-d_2 anhydride was placed into the cell, and the cell was heated to about 320 K and pumped for 30 min with a glass vacuum system and a liquid nitrogen cooled trap. The spectra were measured at several temperatures. A fast decomposition was observed for temperatures above the melting point (392.7 K), leading probably to formation of acrolein and CO_2. The spectrum of the decomposition products, as measured after cooling back to 363 K, was used as a base line to roughly correct for their interference in the high-temperature anhydride vapor spectrum.

Calculational Methods

The X-ray structure of succinic anhydride was taken as representing the starting point for calculation of its minimum energy equilibrium geometry.[15−17] The succinic anhydride molecule has C_{2V} symmetry, within experimental error.[18] The geometry was optimized by energy minimization using the Cadpac program[19] for the SCF and MP2 level calculations and the Gaussian 94 program[20] for the DFT calculations, the latter employing the Becke3LYP exchange-correlation functionals as provided in the program. The Becke hybrid SCF-DFT functional[21] is combined with the Lee−Yang−Parr correlation functional[22] in the B3LYP method. For comparison, a more standard LDA-DFT calculation[23] was also performed. For all these DFT calculations a C_{2V} geometry constraint was applied.

Sets of second derivatives of the energy were calculated analytically at these various levels for use as force fields (FFs) from which sets of vibrational frequencies and normal modes were derived for comparison. To simulate the Raman intensities, the polarizability derivatives were calculated at the SCF/6-31G** level and then were combined with normal mode **S**-vectors obtained from the B3LYP DFT force field. Similarly, local atomic contributions to the atomic axial tensors could only be calculated on the SCF/6-31G** level. The nonlocal parts were calculated from the B3LYP dipolar derivatives using the distributed origin gauge. Complete atomic axial tensors were then combined with the force field and electric dipole derivatives calculated at the DFT level to simulate the VCD.

After the frequency assignment was completed with the frequencies and intensities derived from the *ab initio* FFs above, the frequency agreement could have been further improved by empirically scaling to optimize the frequency agreement,[25] but that has not proven useful in this study. For an estimation of the anharmonic contribution to energies, third and semidiagonal fourth ($d_{\alpha\alpha\beta\gamma}$) derivatives of the energy were calculated by a numerical differentiation of the matrix elements (second derivatives) composing the Cartesian harmonic force field. A step size of 0.005 a_0 was used for the numerical differentiation. The calculation was performed at the SCF/4-31G level, with the SCF/4-31G equilibrium geometry. The harmonic B3LYP/6-31G** force field was transferred to the SCF/4-31G geometry by the method described previously,[5,6,24] so that the B3LYP/6-31G** normal modes could be used to calculate the anharmonic normal mode force constants. The calculation of the SCF anharmonic force field was done using the Cadpac program. At the same time, the first derivatives of the atomic polar and atomic axial tensors were obtained at the SCF/4-31G level.

Similarly, an anharmonic force field using the DFT method at the B3LYP/6-31G level was calculated using Gaussian 94, but a greater step size, 0.01 Å, was required because of the limited numerical accuracy of the DFT methods. The normal mode quartic force field was calculated directly from the *ab initio* Cartesian force field as well as from the Cartesian quartic force field partially corrected for space coordinate invariance, as described in the Appendix.

For the diagonalization of the vibrational Hamiltonian, harmonic oscillator basis functions were used, partially corrected for the diagonal anharmonic terms *via* the phase integrals.[6] The total number of vibrational basis functions was 2011, corresponding to an interaction parameter[5,6] of 0.01 for the SCF/4-31G anharmonic force field; 2082 vibrational basis functions were used for the direct and 2630 for the pretransformed, corrected B3LYP force fields.

Results and Discussion

Geometries and Energies. In Table 1, selected geometry parameters are listed for the calculations and compared to published experimental X-ray structures. Results from two independent experimental determinations are listed, Ehrenberg's early structure[16] with an *R*-factor of 0.076 and that of Fodor et

TABLE 1: Succinic Anhydride Geometry Parameters[a]

method: basis:	SCF 631G**	LSD 631G**	MP2 631G**	B3LYP 631G**	B3LYP 631G**	X-ray[b]	X-ray[c]
C−H	1.083	1.102	1.088	1.094	1.093	1.050	1.035
C−C	1.526	1.511	1.520	1.538	1.530	1.490	1.512
C−CO	1.514	1.504	1.516	1.521	1.522	1.485	1.475
C═O	1.173	1.197	1.203	1.215	1.196	1.168	1.190
CO−O	1.357	1.381	1.394	1.420	1.390	1.385	1.378
O═CO−O	122.1	121.7	121.8	121.6	121.7	120.3	119.3
CO−O−CO	113.0	111.5	111.1	111.2	111.8	111.1	110.1

[a] Bond lengths in Å, bond angles in deg. [b] Reference 15, *R*-factor of 0.076. [c] Reference 16, *R*-factor of 0.032.

TABLE 2: Anhydride Calculated Electronic Energies (in atomic units)

SCF/6-31G**	−378.427 652
MP2/6-31G**	−379.508 293
DFT-LDA/6-31G**	−378.557 501
DFT-B3LYP/6-31G	−380.387 570
DFT-B3LYP/6-31G**	−380.528 708

al.,[17] a more recent structure with an *R*-factor of 0.032. The *ab initio* values generally compare well with experiment, within the experimental error bars.[18] The SCF-calculated structure deviates the most from experiment: the CO−O−CO angle is about 2° larger, and the CO−O bond length is about 0.04 Å smaller, as compared to the experimental values. The SCF and DFT methods have the most error for the length of the C−CO bond which is overestimated by 0.03−0.05 Å in all of the calculations reported here. We expect that the accuracies of the DFT and MP2 methods are quite high and that for further comparison of theoretical and experimental geometries one would need more precise experimental parameters based on the gas phase molecular structure, as obtained, for example, from analysis of the rotational constants. Our resolution limits do not permit such a study.

Although the adiabatic molecular energies listed in Table 2 should be approaching a common limit, few conclusions can be drawn from a direct comparison of the values, because of the quite different theoretical bases of the orbital and density functional methods. Nevertheless, the energies listed do provide a mark for any future calculations on this molecule. For purposes of comparison, the LDA/6-31G** calculation of second derivatives took roughly half the time for the more accurate B3LYP/6-31G** calculation with the same level of basis, while the similar MP2/6-31G** would have been roughly an order of magnitude longer.

Frequency Assignment. The fundamental vibrational frequencies computed with our different force fields are listed in Table 3 for the *trans*-d_2 isotopomer. The modes are ordered according to their frequencies in the MP2 calculation. The MP2 frequency of the lowest energy ring-twisting mode is imaginary (marked as negative in the table). While this implies a problem with the shallow potential for this coordinate, on the basis of the experimental data and the results from other calculations, we believe that the C_{2V} geometry of the parent succinic anhydride still best represents the equilibrium structure. The MP2 method is known to require very large bases for the best performance.[25] For example, we showed previously[6] that the MP2 frequency for the out of plane wagging of the N atom in formamide is imaginary in the 6-31G** basis and becomes real only when an extended basis is used. Moreover, the value of

TABLE 3: Fundamental Frequencies of *trans*-Succinic-d_2 Anhydride[a]

mode, symm.	SCF 631G**	LSDA 631G**	B3LYP 631G	B3LYP 631G**	MP2 631G**	IR solid	IR gas	Raman
1 B	3273	3061	3121	3117	3208	2963	2979	2971
2 A	3269	3057	3116	3112	3203			
3 A	2408	2249	2291	2290	2357	2202	2216	2240
4 B	2403	2246	2289	2287	2353			2200
5 A	2145	1947	1860	1951	1934	1864	1870	1858
6 B	2067	1879	1784	1881	1869	1792	1813	1787
7 A	1455	1277	1364	1340	1381	1292	1305	1291
8 B	1413	1235	1337	1302	1340			
9 B	1396	1214	1302	1270	1304	1258	1251	1258
10 A	1415	1251	1297	1274	1302	1232		1227
11 A	1378	1207	1171	1231	1263	1225	1229	1227
12 A	1204	1102	1113	1113	1155	1085	1105	1096
13 B	1252	1077	1075	1085	1119	1069	1071	1068
14 B	1120	977	975	988	1000	960	963	964
15 A	1058	916	971	954	967	930	926	942
16 B	994	873	871	893	900	885	885	
17 A	919	838	875	856	883			845
18 A	866	800	785	794	810	793	790	797
19 B	795	708	748	730	747		723	724
20 B	714	642	648	650	655	648	668	652
21 A	685	619	612	623	624		635	630
22 B	575	523	529	530	536	534	536	535
23 A	558	493	504	510	515			510
24 B	532	463	491	484	490	470	469	479
25 A	439	390	386	396	398	406	408	408
26 B	151	136	138	137	136			151
27 A	31	50	60	50	-56			
a[b]	1.106	1.013	1.025	1.032	1.055			
Δ/cm^{-1} [b]	129	30	32	33	55			

[a] Frequencies in cm^{-1}; mode symmetry is indicated (C_2 symmetry group). [b] Statistical parameters: *a* corresponds a fit of calculated and experimental frequencies, $\omega_{CAL} = a\omega_{EXP}$; Δ (cm^{-1}) is the root-mean-square deviation.

TABLE 4: Scaling and Anharmonic Corrections to the Harmonic B3LYP Force Field of *trans*-Succinic-d_2 Anhydride[a]

	harmonic[b]		anharmonic[c]				
mode	ω_{harm}	ω_{MP2}	ω^{DFT}_{per}	ω^{SCF}_{var}	ω^{DFT}_{var}	ω^{DFT}_{var}*	ω_{EXP}
1 B	3117	3208	2951	3032	3019	3008	2971
2 A	3112	3203	2959	3006	2996	2948	
3 A	2290	2357	2211	2246	2228	2229	2243
4 B	2287	2353	2174	2264	2255	2240	
5 A	1951	1934	1925	1948	1956	1954	1858
6 B	1881	1869	1872	1887	1890	1890	1787
7 A	1340	1381	1275	1334	1332	1398	1363
8 B	1302	1340	1245	1308	1306	1392	1291
9 B	1270	1304	1183	1244	1218	1251	1250
10 A	1274	1302	1236	1229	1254	1204	1232
11 A	1231	1263	1187	1212	1212	1185	1225
12 A	1113	1155	1103	1084	1105	1088	1090
13 B	1085	1119	1047	1060	1070	1070	1068
14 B	988	1000	957	976	980	1002	964
15 A	954	967	907	929	928	947	942
16 B	893	900	869	885	895	886	885
17 A	856	883	824	845	839	831	849
18 A	794	810	768	794	801	794	795
19 B	730	747	688	702	700	743	724
20 B	650	655	622	644	648	631	648
21 A	623	624	605	635	637	620	630
22 B	530	536	512	537	533	512	535
23 A	510	515	469	482	479	513	510
24 B	484	490	430	461	463	503	479
25 A	396	398	387	416	413	431	408
26 B	137	136	136	162	161	167	151
27 A	50	-56	32	200	175	325	
a	1.032	1.055	0.99	1.013	1.011	1.011	
Δ/cm^{-1}	33	55	34	22	23	30	

[a] Frequencies in cm^{-1}. [b] ω_{harm} are B3LYP/6-31G** frequencies; ω_{MP2} are MP2/6-31G** frequencies. [c] Anharmonic force fields (created by corrections applied to B3LYP/6-31G** harmonic force field): ω^{DFT}_{per} B3LYP/6-31G, perturbational calculation; ω^{SCF}_{var}, ω^{DFT}_{var}, and ω^{DFT}_{var}* variational calculations for the SCF/4-31G, B3LYP/6-31G, and transformed B3LYP/6-31G anharmonic force field, respectively.

the second derivative of the energy had little influence on the vibrational energy in that case, since the potential of the lowest mode of formamide was dominated by a quartic term. The same argument should apply to the succinic anhydride where slightly puckered conformations with low energies will make the potential along the torsional coordinate broad and flatter, thus requiring a substantial quartic contribution. Except for the lowest and experimentally nonassigned modes, the MP2 frequencies are higher by 5.5% than the experimental values on the average. This value is determined from fitting the theoretical to the experimental frequencies with a linear regression whose slope is *a* as given in Table 3. The value of *a* could be viewed as a uniform scaling constant for the force field if one chose to use it in that manner. Statistically, this 5.5% shift up of the MP2 frequencies corresponds to a root-mean-square (rms) deviation, Δ, of 55 cm^{-1} from the experimental values. By contrast, the SCF frequencies are on average 11% higher than the experimental values with $\Delta = 129$ cm^{-1}. Additionally, the SCF ordering of modes 12,13 and 9,10 are switched, as compared to their relative positions in the MP2 calculation.

The B3LYP/6-31G** harmonic frequencies are closer to the experimental values than either the SCF or MP2 results, being on average overestimated by 3.2% with a mean deviation of 33 cm^{-1}. For the lower frequency modes, i.e. those not significantly affected by anharmonic corrections, the experimental values are matched to within an error of only a few wavenumbers. The mode ordering of the modes 9,10 is different than for the MP2 calculation, the energy difference between the two modes being smaller than our ability to separate experimental bandwidths. Surprisingly, the B3LYP calculation in the smaller, 6-31G basis set yields results of almost the same quality in terms of Δ, but a slightly smaller *a* value. This is totally due to the C═O stretch being calculated ~100 cm^{-1} too high in the larger basis set, a trend we have noted in other molecules.[15,26]

In Table 4, harmonic and anharmonic frequencies are compared, on the basis of the B3LYP/6-31G** force field. Anharmonic corrections added *via* perturbational calculation (ω^{DFT}_{per}) do not lead to a smaller rms error, but, in terms of a linear fit (one-point scaling), the ω^{DFT}_{per} frequencies are on average lower by 1% than the experimental values, while the harmonic frequencies are 3.2% higher. The lack of improvement in rms error can be attributed to Fermi resonances not included in the perturbational calculation. Indeed, a variational diagonalization of the vibrational Hamiltonian leads to a smaller rms error of frequencies, for both the SCF and the B3LYP anharmonic force fields. The ω^{SCF}_{var} and ω^{DFT}_{var} frequencies were calculated using the *ab initio* quartic force fields calculated at the SCF/4-31G and B3LYP/6-31G levels, respectively. The invariance transformation of the Cartesian quartic force field (see Appendix) leads to a rather high rms error (corresponding to the set of frequencies we have labeled as ω^{DFT}_{var}*). Nonetheless, many experimental frequencies actually have values that lie between the ω^{DFT}_{var} and ω^{DFT}_{var}* values.

Intensities. By comparison, less accuracy was achieved for the calculation of spectral intensities. Firstly, there are fundamental difficulties in obtaining absolute intensities experimentally, even for solution spectra. An attempt was made to measure the VCD spectrum of the gas phase, but this did not yield quantitatively useful intensities because of the decomposition of the compound at the temperature needed to attain sufficient pressure to develop adequate absorption strengths. Secondly, a higher level of calculation is generally required for calculation of intensity parameters. Nevertheless, for the IR absorption, Raman intensity, and VCD sign pattern, a reasonable agreement with experiment was achieved.

The results for the fundamental mode intensities are summarized in Table 5. While the overall intensity pattern is similar for the SCF and DFT calculations, some difficulties result for

TABLE 5: Spectral Intensity Parameters for (2*S*,3*S*)-Succinic-*2,3*-d_2 Anhydride[a]

	SCF/6-31G**			B3LYP/6-31G** harmonic			B3LYP/6-31G** anharmonic			MP2/6-31G**	
mode[b]	*D*	*R*[c]	Ram	*D*	*R*[c]	Ram	*D*	*R*[c]	Ram	*D*	*R*[c]
1B CHstr	9	0	47	7	−1	47	13	0	30	4	−2
2A CHstr	0	−3	103	0	0	102	0	−1	10	0	0
3A CDstr	0	−1	54	0	−1	53	0	−1	19	0	−1
4B CDstr	8	7	22	5	7	22	6	3	10	4	6
5A COstr	292	−1	19	212	−1	20	132	0	15	144	−1
6B COstr	1604	9	6	1244	5	6	881	13	4	1041	4
7A CH/Db	122	73	5	57	49	5	67	44	4	41	42
8B CH/Db	82	−80	3	4	2	8	2	0	4	3	−3
9B CH/Db	61	11	5	42	−49	7	62	−34	3	54	−44
10A CH/Db	52	−36	1	113	7	2	146	15	1	24	5
11A O−COstr	134	−6	3	565	−27	2	232	−15	1	607	−15
12A C−Cstr	8	−16	5	3	−10	5	1	−4	2	12	−20
13B O−COstr	1270	145	0	873	199	0	748	139	4	891	162
14B O−COstr	300	−70	1	758	−175	0	530	−131	4	848	−113
15A ring def oop	0	2	1	0	− 5	1	1	−10	1	1	2
16B C−COstr	49	−24	1	122	13	1	52	0	0	224	−3
17A C−Cstr	4	3	8	8	4	7	5	−7	7	8	4
18A breathing	14	−5	10	6	−3	10	6	−2	7	12	−5
19B ringdef oop	90	21	2	66	1	1	72	8	2	56	8
20B ring def ip	237	−40	2	268	−14	2	248	−17	2	230	−35
21A CO−O−COb	5	−1	6	7	−1	5	7	0	5	4	−1
22B C═Ob, ip	31	−10	2	27	−11	2	28	−16	2	49	−20
23A ring def oop	0	−3	3	0	−1	3	0	−1	2	0	−1
24B ring def oop	86	28	1	37	20	6	23	21	0	46	37
25A C═Ob ip	200	5	2	122	3	2	127	3	2	119	3
26B chair	131	0	0	110	0	0	106	1	0	86	0
27A ring twist	0	0	0	0	0	1	0	0	0	0	0

[a] *D* and *R*: dipolar and rotational strengths, in 10^{-4} and 10^{-8} D^2, respectively. Ram: Raman intensity in relative units. [b] Abbreviations used for the mode chacteristics: str, stretching mode; b, bending mode; oop, out of plane; ip, in plane (approximately in plane of the ring); def, deformation. [c] SCF/6-31G** atomic axial tensor used for all calculations.

a few modes. For example, the absorption intensity of the 11th mode is about four times higher in the DFT and MP2 calculations than in the SCF, while the 10th mode is much weaker in the MP2 than the DFT and the 16th is much stronger. The most dramatic changes, however, are observed for the VCD intensity, as can be seen by comparing the rotational strengths for the modes 8, 9, 10, and 16, where even the signs predicted with the SCF and DFT force fields are not in agreement. The anharmonic effects can substantially change the harmonic intensities, but dramatic effects are only seen for a few transitions (e.g. mode 5, 6, 11, 16). For the C−D and C−H stretches, the electric dipole second derivatives substantially contribute to the predicted transition dipole strengths of the combination and overtone bands.

In Figure 1 the absorption for the C−D and C−H stretching region of succinic-d_2 anhydride is shown. It is expected that the B symmetry modes will dominate the experimental spectra, because of the very small calculated intensity for the A symmetry modes. The C−H stretching mode (∼3000 cm^{-1}) is not accompanied by resonance modes that would significantly contribute to the absorption intensity, as confirmed by the experiment as well as by the anharmonic calculation (Figure 1b). On the other hand, the anharmonic interaction of the C−D stretching mode (∼2200 cm^{-1}) with higher excited states leads to a very complicated intensity pattern in this spectral region, as seen both in the simulated anharmonic spectrum as well as in the gas and solution phase experimental spectra. Several combination bands result with quite high predicted intensities, and although there is not a simple one-to-one correspondence, several experimental features have moderate intensity in this region, especially as compared to the weak fundamental bands. Also, the CO_2 stretching absorption pattern interferes with the C−D stretching region. Within the accuracy of the calculation and the experimental resolution, assignment of individual frequencies is not possible in this region.

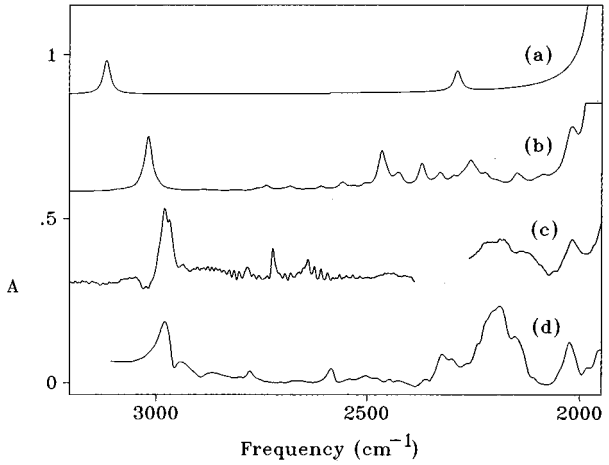

Figure 1. Computed and experimental absorption spectra over the C−H and C−D stretching regions. (top to bottom) Results from the (a) B3LYP/6-31G** calculation; (b) double-anharmonic calculation (B3LYP/6-31G anharmonic force field and SCF/4-31G dipolar second derivatives); (c) gas phase experiment, (resolution 0.1 cm^{-1}, but subsequently smoothed to improve S/N, temperature 415 K; the cut in the spectrum from ∼2300−2400 cm^{-1} is due to CO_2 interference, and the spectral features between 2550 to 2850 cm^{-1} are due to a product from the decomposition of the succinic anhydride); (d) solution phase experiment (combination of two spectra for which acetone and deuterated acetone were used as solvents). Spectrum c has been expanded by about 10-fold to show these features on the same scale used for d, while a and b are plotted on an arbitrary scale. Lorentzian bands with a uniform bandwidth of 10 cm^{-1} were used for the simulated spectra.

The mid-IR absorption is shown in Figure 2. There is a solvent shift down in frequency for the C═O stretching modes, 6 cm^{-1} for the A mode and 21 cm^{-1} for the B mode, but the other mid-IR bands match well between gas and solution phases, other than broadening due to the gas phase rotational contour. As discussed in ref 7, the B symmetry coupled C═O stretching mode stabilizes electronic resonance structures like $O^{(-)}$−

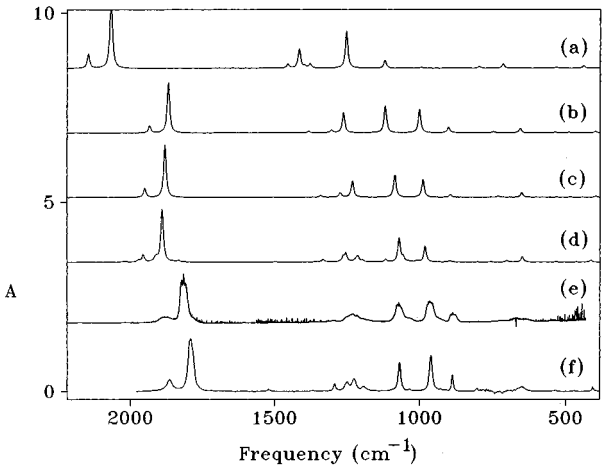

Figure 2. Computed and experimental absorption spectra, in the mid-IR region. (top to bottom) Results from the (a) SCF/6-31G** calculation; (b) MP2/6-31G** calculation; (c) B3LYP/6-31G** calculation; (d) double-anharmonic calculation; (e) the gas phase experiment (resolution 0.1 cm^{-1}, temperature 400 K; residual sharp features from 1800 to 1300 cm^{-1} and below 500 cm^{-1} are due to water vapor which cannot be adequately subtracted out because of the high temperature); (f) solution phase experiment (combination of the two spectra for which $CHCl_3$ and $CDCl_3$ were used as solvents).

C═O$^{(+)}$−C═O and thus can be more affected by the solvent than is the A symmetry mode. As apparent, the C−H/C−D bending region (1100−1400 cm^{-1}) is very difficult to simulate theoretically, since those modes are the ones most affected by anharmonic interactions in the mid-IR. On the other hand, below 1100 cm^{-1} the experimental frequencies and IR absorption intensities are well matched by the calculations. This holds with the exception of the intensity of the mode 16, the B symmetry C−C═O stretch, which is underestimated in all calculations. The anharmonic corrections provide the spectra with more detailed structure whose intensity distribution can be compared to the minor bands seen experimentally, but the global intensity pattern is similar in all the calculations with the exception of the SCF/6-31G**. The frequency shifts in this lower level calculation make comparison with experiment more difficult and result in some modes having a different mixing of motions along local internal coordinates which presumably results in their having different intensities.

For Raman spectra, calculated and experimental spectra for transitions which correspond to the "mid-IR" region are shown in Figure 3. Those bands arising from solvent interference in the experimental spectrum are marked with an asterisk (*) in the lower trace (Figure 3d). Higher concentrations of the anhydride were needed for measurement of the Raman spectrum than were needed for the IR absorption experiment. This led to some shifts of the acetone solvent bands, which consequently could not be properly subtracted from the Raman spectrum of the anhydride solution. The overall intensity pattern is qualitatively reproduced by the calculations in terms of identifying the most intense features and the relative intensities of close lying modes. The major problem was an underestimation of the extremes of intensity, e.g. the very intense (comparatively) features at ∼630 and 800 cm^{-1} with respect to the features near 500 cm^{-1} (Figure 3d). In general the anharmonic corrections (Figure 3c) lead to a more realistic intensity distribution in the C−H deformation modes, if not the low-energy ones. The relative intensity ratio of the two C═O stretching modes is reproduced in all the calculations, but the anharmonic corrections to the FF lead to their being underestimated. A rigorous anharmonic calculation would require polarizability second derivatives which would presumably better represent the underestimated C═O stretching intensities as well as those of

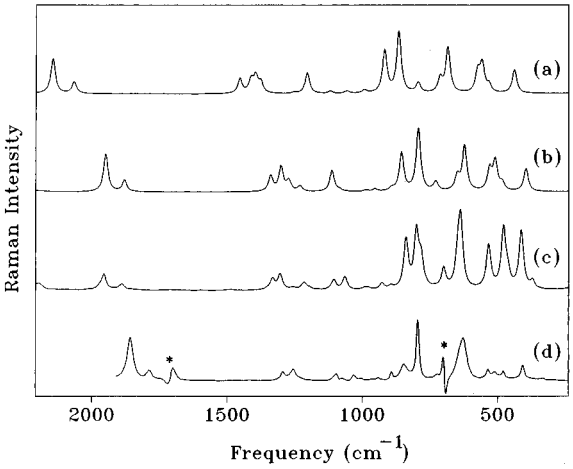

Figure 3. Raman spectra for transitions corresponding to the mid-IR region. (top to bottom) Results from the (a) SCF/6-31G** calculation; (b) B3LYP/6-31G** force field + SCF/6-31G** polarizability derivatives; (c) anharmonic calculation (energies only); (d) experiment (inadequate subtraction of interfering solvent bands led to features marked by *).

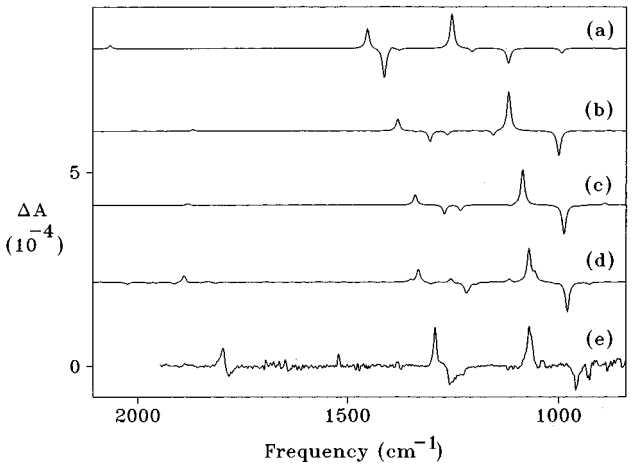

Figure 4. VCD spectra for the (2*S*,3*S*)-succinic-*2,3*-d_2 anhydride. (top to bottom) Results from the (a) SCF/6-31G** calculation; (b) MP2/6-31G** calculation; (c) B3LYP/6-31G** calculation; (d) B3LYP anharmonic corrected calculation; (e) solution phase experiment (formed as a combination of the spectrum for the C═O stretching band and two mid-IR VCD spectra for which $CHCl_3$ and $CDCl_3$ were used as solvents). Experimental results are corrected for an experimental enantiomeric excess of 65%.

the breathing mode (797 cm^{-1}) and the O═C−O−C═O deformation mode (630 cm^{-1}). Considering the lower level of theory for these Raman calculations (i.e. only SCF level polarizability derivatives were used), agreement between simulated and experimental spectra can be considered to be satisfactory.

The computed and experimental VCD spectra (scaled to correct for 65% enantiomeric excess) for (2*S*,3*S*)-succinic-*2,3*-d_2 anhydride are shown in Figure 4. We were unsuccessful in detecting the very weak predicted C−H and C−D stretching VCD even though our instrument has measured such spectra with good S/N for other compounds.[26] The overall experimental VCD sign pattern is generally replicated by the calculations, but there are significant intensity and frequency variations between the spectra in Figure 4. All the intense fundamental bands are predicted with the correct signs by the MP2, DFT, and DFT anharmonic calculations. The anharmonic force field somewhat improves the intensity pattern, giving rise to a more intense C═O stretching VCD, as well as predicting a small intensity for the B symmetry $|23^{1}24^{1}\rangle$ overtone at 1035 cm^{-1} (calculated at 1053 cm^{-1} as a shoulder on the fundamental to

TABLE 6: Becke3LYP Force Field: Deuterated Isomers of Succinic Anhydride[a]

mode	d_0:ω	ω_{exp}[b,d]	D	d_1: ω	D	d_2/*trans* ω	D	d_2/*cis* ω	D	d_3:ω	D	d_4:ω	ω_{exp}[c,d]	D
1	3142 B1	(2975)	2	3136	2	3117 B	7	3120 A′	1	3115	3	2327 B1	(2185)	2
2	3128 A2	(2975)	0	3114	2	3112 A	0	3110 A″	6	2325	1	2323 A2	(2185)	0
3	3095 A1	(2975)	0	3093	7	2290 A	0	2291 A′	2	2289	2	2257 A1	(2185)	1
4	3091 B2	(2975)	12	2288	3	2287 B	5	2286 A″	4	2253	4	2249 B2	(2185)	7
5	1951 A1	1868	214	1951	213	1951 A	212	1951 A′	212	1950	211	1950 A1	1852	211
6	1881 B2	1790	1243	1881	1244	1881 B	1244	1881 A”	1244	1881	1244	1881 B2	1790	1244
7	1490 A1	1425	51	1479	29	1340 A	57	1329 A′	61	1322	38	1246 A1	1267	691
8	1467 B2	1405	1	1324	30	1302 B	4	1320 A″	4	1273	93	1186 A1	1232	1
9	1320 B2	1300	26	1311	40	1274 A	113	1282 A″	25	1239	603	1159 B2	1149	354
10	1304 A1	1280	76	1277	84	1270 B	42	1269 A′	215	1170	97	1080 A1	1057	32
11	1253 A2		0	1233	574	1231 A	565	1227 A′	461	1107	326	1074 B2	1088	8
12	1233 A1	1225	609	1203	17	1113 A	3	1092 A″	830	1061	348	1012 B2	970	1349
13	1167 B1		10	1093	424	1085 B	873	1067 A′	10	999	893	940 B1		40
14	1070 B2	1049	1276	1056	807	988 B	758	995 A″	662	958	35	939 A2		0
15	1031 A2		0	995	31	954 A	0	958 A″	158	927	22	918 A2		0
16	1024 A1	1010	24	948	414	893 B	122	904 A′	40	885	86	876 B2	872	66
17	927 B2	905	459	895	100	856 A	8	888 A″	92	844	11	816 A1		4
18	828 B1		75	804	5	794 A	6	795 A′	8	783	9	770 A1	770	10
19	812 A1	815	3	758	59	730 B	66	699 A′	51	683	57	657 B1		55
20	662 B2	652	276	656	273	650 B	268	651 A″	269	644	259	637 B2	630	256
21	624 A1	629	7	624	7	623 A	7	623 A′	8	622	9	621 A1	629	8
22	553 B2	562	39	546	22	530 B	27	541 A″	20	524	26	512 B2	520	38
23	546 B1		37	539	22	510 A	0	500 A″	15	480	13	485 A2		0
24	544 A2		0	498	25	484 B	37	488 A′	30	464	26	450 B1		29
25	398 A1	412	121	397	121	396 A	122	396 A′	122	395	123	394 A1	412	124
26	137 B1		113	137	112	137 B	110	137 A′	110	137	110	137 B1		109
27	64 A2		0	50	3	50 A	0	47 A″	0	45	2	43 A2		0

[a] Symbols and units same as in previous tables. [b] $a = 1.041$, $\Delta = 30$ cm^{-1}. [c] $a = 1.034$, $\Delta = 28$ cm^{-1} (see Table 3 for the meaning of statistical parameters; C−H/C−D stretching modes were not included for calculation of Δ). [d] Experimental frequencies for gas phase samples, from ref 8.

lower energy; its symmetry can also be identified from its rotational overlap in the gas phase spectrum) and the 15th fundamental mode at 930 cm^{-1} (calculated weakly negative at 928 cm^{-1} for the anharmonic approach). On the other hand, the VCD signal of the overtones calculated between 1330 and 1220 cm^{-1} cannot be identified in the experimental spectrum so that the harmonic approximation better describes the intensity pattern in the C−H/C−D deformation region (experimental VCD bands 1293, 1254, and 1224 cm^{-1}, harmonic B3LYP 1340, 1270, and 1231 cm^{-1}, anharmonic B3LYP 1332, 1218, and 1212 cm^{-1}).

Despite minor differences in detail between the computed and experimental VCD spectra, it is clear that the absolute stereochemistry of the *trans*-succinic-d_2 anhydride is established to be (2*S*,3*S*) by theoretical simulation of this spectral measurement. This compound does not have an easily measurable electronic CD nor is its rotation related to its absolute configuration in a straightforward manner. Our experimental confirmation of its configuration and deuteration pattern was dependent on rehydrolysis to the acid form, for which there happened to be available earlier CD data referenced *via* a series of synthetic steps to known compounds.[12,27] For a less well-referenced compound with a stable conformation, these results show that computation of the VCD spectral pattern and comparison to experimental data offer a viable means of absolute stereochemistry determination. Even for the simplest calculation done here, at the SCF/6-31G** level, the overall mid-IR VCD pattern calculated when compared to the experimental data eliminates any doubt as to the absolute configuration.

The frequency (ω) and dipole strength (D) values for all possible deuteration patterns of the succinic anhydride were also computed with the B3LYP force field and atomic polar tensors and are listed in Table 6. Comparison with experimental IR data for the d_0 and d_4 isotopomers[8] indicates a similar level of agreement with experiment as found above for the *trans*-d_2 isotopomer. Many “skeletal” modes are almost unaffected by deuteration, since, as expected, the biggest changes of experimental frequencies and intensities are predicted for the C−H/C−D stretching and bending regions. For example, the CH(CD) bending mode of highest frequency (and of highest symmetry) is calculated at 1490 cm^{-1} for the d_0 isomer. Its frequency decreases with the degree of deuteration, to 1479 cm^{-1} for the d_1 isomer, 1340/1329 cm^{-1} for the *trans/cis*-d_2 isomers, and, finally, 1322 and 1246 cm^{-1} for the d_3 and d_4 isomers, respectively. Considering the agreement between the calculated and experimental frequencies for the d_0, d_4, and *trans*-d_2 isomers, it should also be possible to use vibrational spectroscopy to determine isotopic substitution patterns, if combined with *ab initio* calculations. Caution should be paid, however, to the anharmonic effects.

Our results are consistent with those of Rauhut and Pulay,[25] who used the B3-LYP/6-31G** force field to develop a transferable scaled force field from calculations for a training set of 20 organic molecules. They found that the method consistently overestimates the harmonic frequencies by about 5%. Also, their rms error of 13 cm^{-1} compares well with our error of 15 cm^{-1} from scaling the B3-LYP/6-31G** force field. Further correction should account for anharmonic effects as we have attempted to do in this work for other reasons. Also, the solvent shift should be taken into account for an objective comparison of experimental frequencies and intensities. As seen in the figures, the gas−solvent shift is not a constant and affects different modes uniquely. Similarly, the improvement in VCD prediction accompanying the improved FF characteristic of the B3LYP/6-31G** calculations is consistent with the results of Stephens and co-workers on a series of smaller model compounds.[4,28]

Conclusions

Experimental IR absorption, Raman, and VCD frequencies and intensities were well reproduced on the basis of *ab initio* calculations that included some level of CI correction, MP2 or DFT. Anharmonic corrections added more detailed structure to the intensity distribution of the computed spectra making the simulations more realistic. The C═O and C−D stretching modes are most affected by anharmonic interactions with lower

frequency modes, while the lowest energy, ring-twisting mode potential is dominated by a quartic term. The DFT methods proved to be suitable not only for calculation of the harmonic force field but also, if combined with atomic polar tensors implemented on the SCF level, as has been proposed by Stephens,[4] result in a very satisfactory representation for the VCD intensities.

Acknowledgment. Work at UIC was supported in the past by NSF grants (CHE 88-14105 and INT 91-07588) and by a University of Illinois Senior Scholar Award to T.A.K.; P.B. was supported by the grant of the Academy of Sciences of the Czech Republic (203/95/0105), and C.N.T. by a Dean's Scholar Fellowship and the Philip L. Hawley Fellowship of the University of Chicago at Illinois. P.B. thanks Dr. Jana Sopkova for discussion of the X-ray structure, and T.A.K. thanks Prof. Philip Stephens for preprints of unpublished work.

Appendix: Invariance of Quartic Force Field

An incomplete quartic force field obtained by the differentiation of the *ab initio* harmonic force field does not obey rotational and translational invariance (for these six spatial coordinates). During transformation to a normal mode force field, the rotational and translational components should not alter the vibrational frequencies for a complete force field, because the space and normal mode coordinates are orthogonal. The following procedure projects out the spatial coordinate part of the force field before the Cartesian−normal mode transformation, leading to slightly different normal mode force field.

Let us define a new quartic force field $\mathbf{d}'$ as

$$\mathbf{d}'_{\alpha\beta\gamma\delta} = a_{\alpha\alpha'}a_{\beta\beta'}a_{\gamma\gamma'}a_{\delta\delta'}d_{\alpha'\beta'\gamma'\delta'} \quad (1)$$

with $\mathbf{d}$ being the incomplete force field. The projection matrix $\mathbf{a}$ is defined as[19]

$$\mathbf{a} = \mathbf{E} - \mathbf{s}\cdot\mathbf{s}^{t} \quad (2)$$

where $\mathbf{E}$ is a unit matrix and $\mathbf{s}$ is a $3N \times 6$ ($3N \times 5$ for linear molecules) matrix where N is the number of atoms. The translation/rotation−Cartesian transformation matrix $\mathbf{s}$ can be calculated by an orthonormalization of the columns of the matrix $\mathbf{s}'$

$$s'_{3(\lambda-1)+j,j} = 1 \text{ for } j = 1...3,\ \lambda = 1...N$$

$$s'_{3(\lambda-1)+k,j} = \sum_{l=1...3} \epsilon_{k,j-3,l}R^{\lambda}_{\ l} \text{ for } j = 4...6,\ k = 1...3,$$
$$\lambda = 1...N; \text{ other } s'_{ij} = 0 \quad (3)$$

The new quartic force field $\mathbf{d}'$ is thus translationally and rotationally invariant. However, the new semidiagonal elements $d'_{\alpha\alpha\gamma\delta}$ differ from the exact values $d_{\alpha\alpha\gamma\delta}$ found by the *ab initio* calculation. Clearly, it is impossible to obtain an accurate rotationally−translationally invariant field from an incomplete set of constants. We used an iterative procedure to partially remove this problem. First we redefined the semidiagonal elements in the new force field as

$$d'_{\alpha\alpha\gamma\delta} = d_{\alpha\alpha\gamma\delta} \quad (4)$$

and then repeated the transformation in eq 1 until the off-diagonal elements did not change. This improved quartic force field was used for a calculation of the normal mode quartic force field $\mathbf{D}$. Note that also only the semidiagonal terms D_{iiii}, D_{iiij}, D_{iijj}, and D_{ijik} of the normal mode force field are used in the second-order perturbation expressions for the vibrational energies.

We used the same projection matrix to improve the invariance of the complete Cartesian cubic force field. In this case, we observed only a negligible change in vibrational frequencies, originating from numerical inaccuracies in the differentiation calculation by finite differences.

References and Notes

(1) Stephens, P. J. *J. Phys. Chem.* **1985**, *89*, 748; **1987**, *91*, 1712. Jalkanen, K. J.; Stephens, P. J.; Amos, R. D.; Handy, N. C. *Chem. Phys. Lett.* **1987**, *133*, 21. Amos, R. D.; Jalkanen, K. J.; Stephens, P. J. *J. Phys. Chem.* **1988**, *92*, 5571.

(2) Malon, P.; Keiderling, T. A.; Uang, J.-Y.; Chickos, J. S. *Chem. Phys. Lett.* **1991**, *179*, 282.

(3) Malon, P.; Mickley, L. J.; Sluis, K. M.; Tam, C. N.; Keiderling, T. A.; Kamath, S.; Uang, J.-Y.; Chickos, J. S. *J. Phys. Chem.* **1992**, *96*, 10139.

(4) Stephens, P. J.; Devlin, F. J.; Ashwar, C. S.; Chabalowski, C. F.; Frisch, M. J. *Faraday Discuss.* **1994**, *99*, 103. Stephens, P. J.; Devlin, F. J.; Chabalowski, C. F.; Frisch, M. J. *J. Phys. Chem.* **1994**, *98*, 11623. Devlin, F. J.; Finley, J. W.; Stephens, P. J.; Frisch, M. J. *J. Phys. Chem.* **1995**, *99*, 16883.

(5) Bour, P. *J. Phys. Chem.* **1994**, *98*, 8862.

(6) Bour, P.; Bednarova, L. *J. Phys. Chem.* **1995**, *99*, 5961.

(7) Mirone, P.; Chiorboli, P. *Spectrochim. Acta* **1962**, *18*, 1425.

(8) di Lauro, C.; Califano, S.; Adembri, G. *J. Mol. Struct.* **1968**, *2*, 173.

(9) Bour, B.; Keiderling, T. A. *J. Am. Chem. Soc.* **1993**, *115*, 9602.

(10) Florian, J.; Johnson, B. G. *J. Phys. Chem.* **1995**, *99*, 5899.

(11) Vogel, A. *A Textbook of Practical Organic Chemistry*, 3rd ed.; Wiley: New York 1966; p 375.

(12) Shaharuzzaman, M; Chickos, J.; Tam, C. N.; Keiderling, T. A. *Tetrahedron*: *Asymmetry* **1995**, *6*, 2929.

(13) Chickos, J. S.; Bausch, M.; Alul, R. *J. Org. Chem.* **1981**, *46*, 3559.

(14) Keiderling, T. A. In *Practical Fourier Transform Spectroscopy*; Krishnan, K., Ferraro. J. R., Eds.; Academic: San Diego, 1990; p 203. Keiderling, T. A. *Appl. Spectrosc. Rev.* **1981**, *17*, 189.

(15) Tam, C. N. Ph.D. Thesis, University of Illinois at Chicago, 1995.

(16) Ehrenberg, M. *Acta Crystallogr.* **1965**, *19*, 698.

(17) Fodor, G.; Sussangkarn, K.; Mathelier, H.; Arnold, R.; Karle, I; George, C. *J. Org. Chem.* **1984**, *49*, 5064.

(18) Laskowski, R. A.; Moss, D. S.; Thornton, J. M. *J. Mol. Biol.* **1983**, *231*, 1049.

(19) Amos, R. D. *CADPAC version 5.0*; SERC Laboratory: Daresbury, U.K., 1984; issue 1990.

(20) Frisch, M. J.; Trucks, G. W.; Schlegel, H. B.; Gill, P. M. W.; Johnson, B. G.; Robb, M. A.; Cheeseman, J. R.; Keith, T. A.; Petersson, G. A.; Montgomery, J. A.; Raghavachari, K.; Al-Laham, M. A.; Zakrezewski, V. G.; Ortiz, J. V.; Foresman, J. B.; Cioslowski, J.; Stefanov, B. B.; Nanayakkara, A.; Challacombe, M.; Peng, C. Y.; Ayala, P. Y.; Chen, W.; Wong, M. W.; Andres, J. L.; Replogle, E. S.; Gomperts, R.; Martin, R. L.; Fox, D. J.; Binkley, J. S.; Defrees, D. J.; Baker, J.; Stewart, J. P.; Head-Gordon, M.; Gonzalez, C.; Pople, J. A. *GAUSSIAN 94*; Gaussian Inc.: Pittsburgh, PA, 1995.

(21) Becke, A. D. *J. Chem. Phys.* **1993**, *98*, 5648.

(22) Lee, C.; Yang, W.; Parr, R. G. *Phys. Rev. B* **1988**, *37*, 785.

(23) Becke. A. D. In *The Challenge of d and f Electrons*; Salahub, D. R., Zerner, M. C., Eds.; American Chemical Society: Washington DC, 1989.

(24) Bour, P.; Sopkova, J.; Bednarova, L.; Malon, P.; Keiderling, T. A. Submitted for publication.

(25) Pulay, P. *J. Phys. Chem.* **1995**, *99*, 3093.

(26) Wang, B.; Keiderling, T. A. *Appl. Spectrosc.* **1995**, *49*, 1347. Tam, C. N.; Bour, P.; Keiderling, T. A. Submitted for publication.

(27) Portsmouth, D.; Stoolmillen, A. C.; Abeles, R. H. *J. Biol. Chem.* **1967**, *242*, 2751.

(28) Stephens, P. J.; Devlin, F. J.; Ashvar, C. S., Bak, K. L.; Taylor, P. R.; Frisch, M. J. *ACS Symp. Ser.*, in press. Cheeseman, J. R.; Frisch, M. J.; Devlin, F. J.; Stephens, P. J. *Chem. Phys. Lett.*, in press. Stephens, P. J.; Ashvar, C. S.; Devlin, F. J.; Cheeseman, J. R.; Frisch, M. J. *Mol. Phys.*, in press.

JP961217B